The EMBO Journal Vol. 22 No. 20 pp. 5412–5421, 2003

Phosphatidylinositol-4,5-bisphosphate, PIP_2, controls KCNQ1/KCNE1 voltage-gated potassium channels: a functional homology between voltage-gated and inward rectifier K^+ channels

G.Loussouarn[1], K.-H.Park, C.Bellocq, I.Baró, F.Charpentier and D.Escande

Institut National de la Santé et de la Recherche Médicale, INSERM U533 Laboratoire de Physiopathologie et de Pharmacologie Cellulaires et Moléculaires, Hôpital Hôtel-Dieu, Nantes, France

[1]Corresponding author
e-mail: gildas.loussouarn@nantes.inserm.fr

Phosphatidylinositol-4,5-bisphosphate (PIP_2) is a major signaling molecule implicated in the regulation of various ion transporters and channels. Here we show that PIP_2 and intracellular MgATP control the activity of the KCNQ1/KCNE1 potassium channel complex. In excised patch–clamp recordings, the KCNQ1/KCNE1 current decreased spontaneously with time. This rundown was markedly slowed by cytosolic application of PIP_2 and fully prevented by application of PIP_2 plus MgATP. PIP_2-dependent rundown was accompanied by acceleration in the current deactivation kinetics, whereas the MgATP-dependent rundown was not. Cytosolic application of PIP_2 slowed deactivation kinetics and also shifted the voltage dependency of the channel activation toward negative potentials. Complex changes in the current characteristics induced by membrane PIP_2 was fully restituted by a model originally elaborated for ATP-regulated two transmembrane-domain potassium channels. The model is consistent with stabilization by PIP_2 of KCNQ1/KCNE1 channels in the open state. Our data suggest a striking functional homology between a six transmembrane-domain voltage-gated channel and a two transmembrane-domain ATP-gated channel.

Keywords: KCNE1/KCNQ1/MgATP/phosphatidylinositol-4,5-bisphosphate

Introduction

The KCNQ1/KCNE1 channel complex underlying the delayed rectifier potassium current, I_{Ks}, is key in controlling the duration of the action potential of the human heart (Barhanin *et al*., 1996; Sanguinetti *et al*., 1996) and also potassium secretion in the endolymphatic space of the inner ear (Vetter *et al*., 1996). Genetic mutations affecting either KCNQ1 (the α-subunit) or KCNE1 (the β regulatory subunit) are responsible for long QT syndrome, a rare, albeit severe, human genetic disorder, and also for congenital deafness (Towbin and Vatta, 2001).

The phospholipid phosphatidylinositol-4,5-bisphosphate (PIP_2) is an important regulator of several ion channels and transporters (Shyng and Nichols, 1998; Hilgemann *et al*., 2001). In particular, PIP_2 has been reported to modulate the voltage dependency of recombinant HERG channels and to stabilize the activity of the voltage-dependent potassium channels HERG and Kv2.1 in excised patches (Bian *et al*., 2001; Hilgemann *et al*., 2001). The KCNQ family of voltage-dependent potassium channels is also regulated by PIP_2 (Suh and Hille, 2002; Zhang *et al*., 2003). The regulation by PIP_2 of the pancreatic ATP-sensitive K^+ channel (constituted by the assembly of Kir6.2 α-subunits and SUR1 proteins), a two transmembrane-domain inward rectifier channel, has been investigated in greater detail (Baukrowitz and Fakler, 2000). In the case of the Kir6.2/SUR1 channels, a model has been established which proposes that PIP_2 stabilizes the open state of the channel, whereas ATP stabilizes the closed state. This model recapitulates many characteristics of the channel biophysics, including its maximum open probability and ATP sensitivity for varying membrane PIP_2 levels and various pore mutations (Enkvetchakul *et al*., 2000).

In the present study, our objective was to investigate whether a common mechanism would underlay regulation by PIP_2 of voltage-gated and inward rectifier potassium channels, despite their different structural characteristics. We demonstrate that PIP_2, but also MgATP, is necessary for maintaining KCNQ1/KCNE1 complex activity. We show that the effects of PIP_2 on the characteristics of the KCNQ1/KCNE1 currents are fully recapitulated by a model derived from the Kir6.2/SUR1 model, in which regulation by voltage (in the case of KCNQ1 α-subunits) replaces regulation by intracellular ATP (in the case of Kir6.2 α-subunits). The model is also consistent with the interpretation that PIP_2 stabilizes the open state of the KCNQ1/KCNE1 channel. Our results suggest a strong functional homology, conserved between a six transmembrane-domain voltage-gated channel (KCNQ1) and a two transmembrane-domain inward rectifier (Kir6.2).

Results

PIP_2-dependent and -independent rundown of KCNQ1/KCNE1 channels

KCNQ1 and KCNE1 channel proteins were co-expressed in COS-7 cells. We first examined the effect of patch excision on channel activity. Because of the small conductance and the possible clustering of the channels (Yang and Sigworth, 1998), sizeable KCNQ1/KCNE1 currents were recorded in only 15% of the cell-attached patches (from 663 successful patches, 106 demonstrated sizeable currents). Figure 1A illustrates a representative inside-out recording after excision in a divalent ion-free high potassium medium. Complete rundown of the channel activity occurred within 5 min (Figure 1B). This time-frame for rundown was very comparable to that observed for endogenous I_{Ks} channels in inner ear epithelial cells (Shen and Marcus, 1998). We did not observe any shift in the leak-subtracted reversal potential,

suggesting that the K^+ selectivity was not modified by rundown. Application at the inner face of the membrane of Mg^{2+} alone or Mg^{2+} plus Ca^{2+} accelerated rundown (Figure 1B and C), similar to the observation previously made by Shen and Marcus (1998) with the native current.

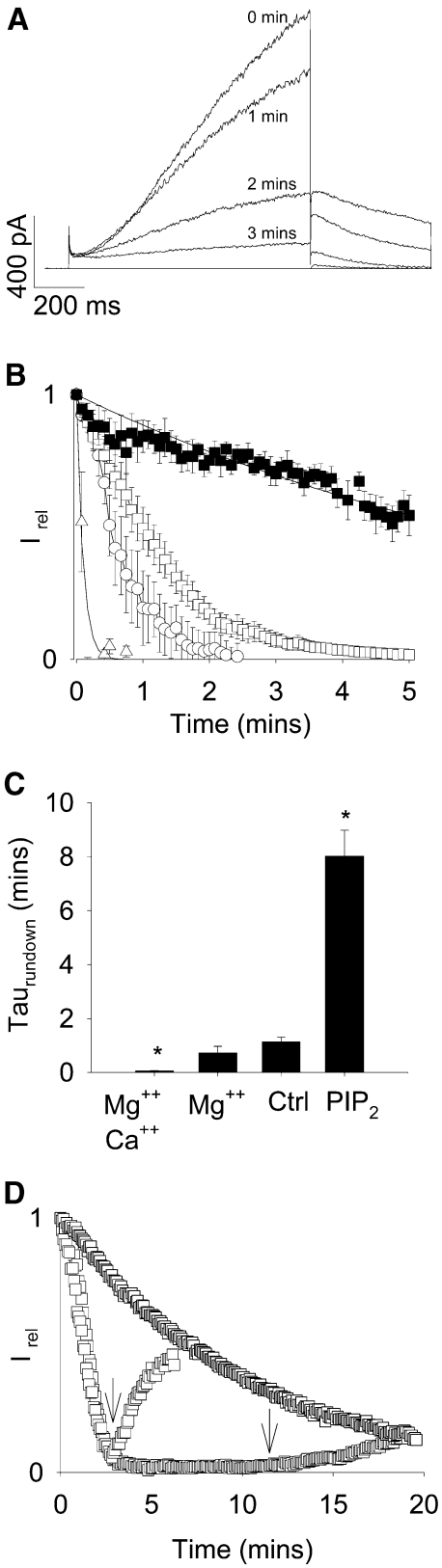

In order to investigate the effects of PIP_2 on channel rundown, PIP_2 (5 μg/ml) was added to the cytosolic solution just prior patch excision. Addition of PIP_2 markedly slowed but did not entirely suppress the rundown (Figure 1B and C). Strikingly, we observed that when we applied PIP_2 after the patch was excised as illustrated in Figure 1D, the current raised up to a level that coincided with a slower rundown curve uncovering a PIP_2-independent rundown phenomenon. A very slow PIP_2-independent rundown exists in the case of Kir6.2/SUR1 channels in the presence of the same concentration of PIP_2 (Shyng and Nichols, 1998).

Because PIP_2 is known to activate actin polymarization (Yin and Janmey, 2003), we hypothesized that KCNQ1/KCNE1 activity could depend on the assembly/disassembly of the actin cytoskeletal network. To test this hypothesis, we investigated the effects of cytochalasin D on the channel activity in the perforated patch condition. Monitoring KCNQ1/KCNE1 activity during application of 10 μM cytochalasin for 10 min did not show any effect of actin depolymerization when compared with control conditions (n = 4 and 6, respectively; data not shown). This is consistent with the absence of effects of cytochalasin on the amplitude of KCNQ1 currents expressed in *Xenopus* oocytes (Grunnet *et al*., 2003). These data suggest that PIP_2 regulation of the channel does not occur through the cytoskeletal network.

PIP_2-dependent rundown, but not PIP_2-independent rundown, is associated with an acceleration in deactivation

In Kir6.2/SUR1 channels, it is well known that variations in membrane PIP_2 levels affect not only the current amplitude, but also the ATP sensitivity of the channel and the single channel kinetics (Enkvetchakul *et al*., 2000). These modifications can be interpreted as resulting from a unique event, i.e. stabilization by PIP_2 of the open conformation of the ATP-controlled gate. If PIP_2 acts on the KCNQ1/KCNE1 complex through stabilization of the open conformation of the voltage controlled gate, a decrease in PIP_2 levels during rundown should be accompanied by changes in the activation and/or deactivation rates, and by a shift of the voltage dependency. It is known that channels made of KCNQ1 and KCNE1 do not exhibit substantial inactivation (Tristani-Firouzi and

Fig. 1. KCNQ1/KCNE1 channel rundown is accelerated by divalent cations and slowed by PIP_2. (**A**) Representative inside-out recording of KCNQ1/KCNE1 currents at various time after excision in a control solution (145 mM K-gluconate, 10 mM K-HEPES, 1 mM K-EGTA, pH 7.2). The membrane potential was stepped from a holding potential of –80 to +40 mV (1000 ms) and then back to –40 mV (500 ms), every 5 s. Zero current is indicated by a solid line. (**B**) Average time-dependent currents measured at the end of the depolarizing step relative to their maximum value and plotted against various times after patch excision. Patches were excised in control solution (open squares, n = 9), control solution plus 0.6 mM free Mg^{2+} (open circles, n = 6), control solution plus 1 mM free Mg^{2+} and Ca^{2+} (open triangles, n = 5) or control solution plus 5 μg/ml PIP_2 (filled squares, n = 5). (**C**) Mean ± SEM values of $\tau_{rundown}$ determined from a monoexponential fit of rundowns in the different conditions presented in (B). *$P < 0.001$ compared with control. (**D**) Individual time-dependent currents measured at the end of the depolarizing step relative to their maximum value measured after patch excision. Three individual traces are presented, one with PIP_2 application just before excision, and two with PIP_2 application at 3 or 12 min after excision (arrows).

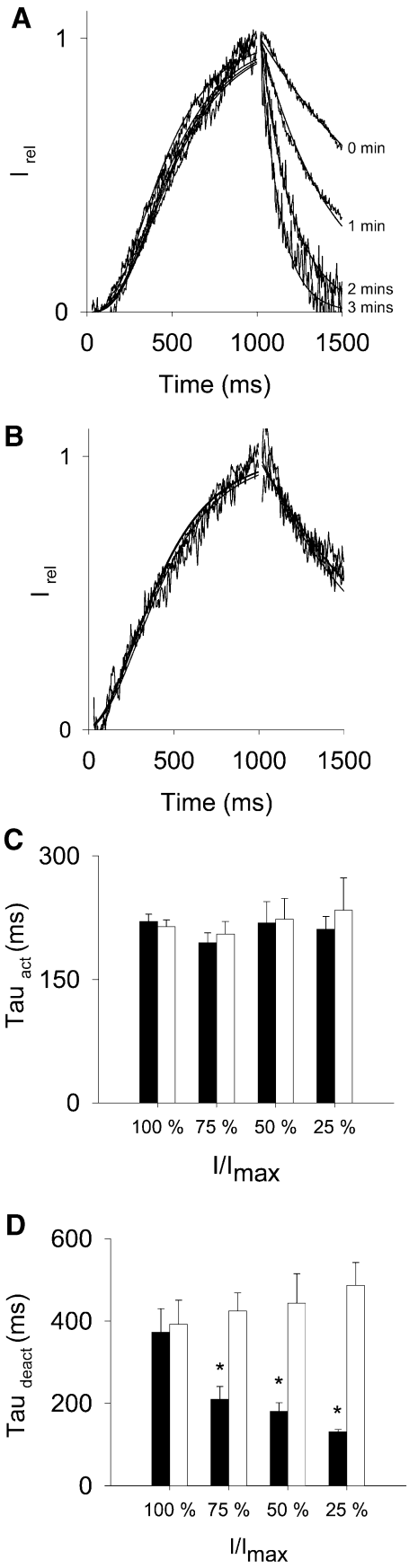

Sanguinetti, 1998). PIP_2-related rundown was too fast to permit accurate measurement of the half-maximum activation potential, $V_{0.5}$. In contrast, the activation/deactivation kinetics could be convincingly quantified. Current traces were normalized during activation (from –80 to +40 mV) and deactivation (from +40 to –40 mV) in the presence and absence of PIP_2. As shown in Figure 2, there was no alteration in the activation kinetics either during PIP_2-dependent or PIP_2-independent rundown (Figure 2C). In contrast, close examination of the tail current revealed that deactivation was markedly accelerated during PIP_2-dependent rundown but not in presence of PIP_2 (Figure 2D). When PIP_2 was added at different times after excision (as in Figure 1D), deactivation initially accelerated (τ_{deact} decreased from 564 ± 230 to 131 ± 9 ms) until PIP_2 was applied. At this point, deactivation slowed, only partially reaching pre-rundown values (τ_{deact} 278 ± 68 ms; $n = 3$). It is likely that PIP_2-independent rundown prevented recording of PIP_2-induced complete recovery of deactivation.

Altogether, these observations confirm the presence of two types of rundown: a PIP_2-dependent rundown associated with accelerated deactivation kinetics and a PIP_2-independent rundown not associated with alteration in activation or deactivation kinetics.

PIP_2-independent rundown is neither okadaic acid nor calmodulin sensitive

We investigated further PIP_2-independent rundown and tentatively prevented this slow rundown process. It is known that KCNQ1/KCNE1 activity is modulated by phosphorylation (Potet *et al*., 2001; Marx *et al*., 2002). Although in our experiments, channels were not expressed with an AKAP (a kinase anchoring protein) to target protein kinase A (PKA) at the vicinity of the channel, a less specific phosphorylation may have occurred. If PIP_2-independent rundown was caused by the activity of a phosphatase, inhibition of this phosphatase should reduce the rundown. Okadaic acid (300 nM), an inhibitor of phosphatase 1 (PP1) and PP2A did not modify either PIP_2-dependent or PIP_2-independent rundown, thereby excluding the involvement of an okadaic acid-sensitive phosphatase (Figure 3A and C). In the yeast two-hybrid assay, different groups, including ours (F.Le Bouffant,

Fig. 2. PIP_2-dependent, but not PIP_2-independent, rundown is associated with an acceleration of the deactivation. (**A** and **B**) Representative normalized inside-out recordings of KCNQ1/KCNE1 currents at various time after excision in the absence (A) or presence (B) of PIP_2 (5 μg/ml). Activating pulse currents measured at different time after excision were normalized to 1 at the end of the depolarizing step, in order to compare activation kinetics (left part of the curve). Deactivating tail currents at different time after excision were normalized to 1 at the beginning of the repolarizing step, so as to compare deactivation kinetics (right part of the curve). (**C**) Mean ± SEM values of τ_{act} determined from a fit of the activating current based on the Hodgkin and Huxley model for a voltage-dependent potassium channel activation (cf. Materials and methods). Black bars (0 μg/ml PIP_2) and white bars (5 μg/ml PIP_2) represent the average τ_{act} as a function of the remaining current during rundown (100, 75, 50 and 25% stand for the ranges 75–100%, 50–75%, 25–50% and 0–25%, respectively (n = 5–16). (**D**) Mean ± SEM values of τ_{deact} measured from a monoexponential fit of the deactivating tail current. Black bars (0 μg/ml PIP_2) and white bars (5 μg/ml PIP_2) represent the average τ_{deact} as a function of the remaining current during rundown (n = 4–16). *$P < 0.01$.

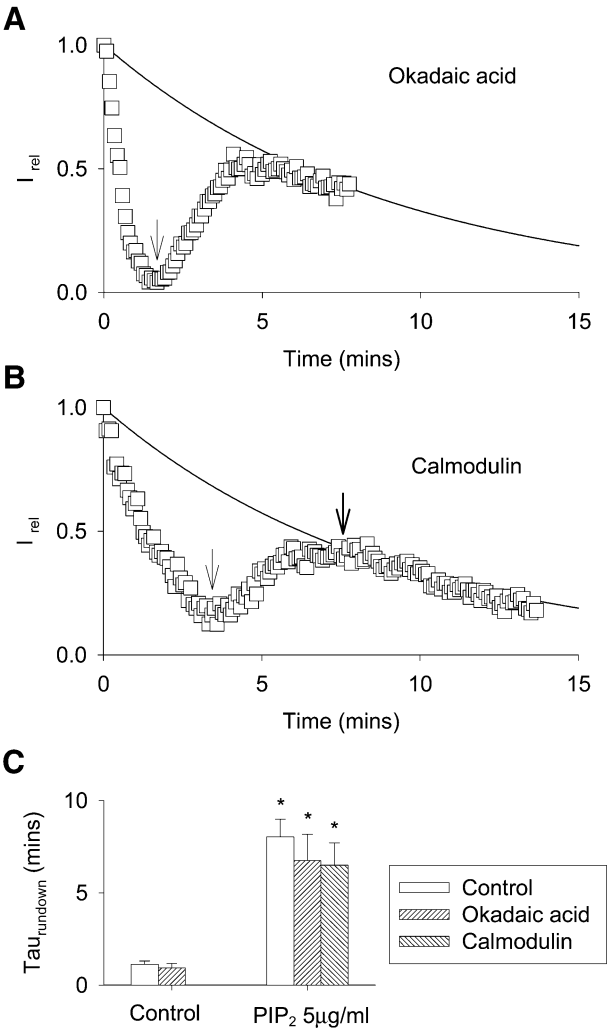

Fig. 3. PIP_2-independent rundown is okadaic acid and calmodulin insensitive. (**A**) Representative PIP_2-dependent and -independent rundowns of the KCNQ1/KCNE1 current in the presence of 300 nM okadaic acid. The KCNQ1/KCNE1 current is calculated as in Figure 1B and D. The arrow indicates PIP_2 application to the cytosolic side of the patch. The solid line represents the average rundown in presence of PIP_2 in control cells. (**B**) Representative PIP_2-dependent and -independent rundown of the KCNQ1/KCNE1 current. The first arrow indicates PIP_2 application to the cytosolic side of the patch, the second arrow indicates 500 nM CaM cytosolic application. The solid line represents the average rundown in presence of PIP_2 in control cells. (**C**) Mean ± SEM values of $\tau_{rundown}$ from a monoexponential fit of rundowns in the different conditions presented in (A) and (B) (n = 5–9). *P < 0.001 compared to control.

I.Baró and D.Escande, unpublished results), found that calmodulin (CaM) interacts with the intracellular C-terminal region of several members of the KCNQ family (KCNQ2, KCNQ3, KCNQ5 and, less clearly, KCNQ1 and KCNQ4; Yus-Najera *et al*., 2002). In KCNQ2/3 channels, Wen and Levitan (2002) demonstrated a correlation between CaM binding and channel function. Although KCNQ1–CaM interactions were possibly weak, we supposed that PIP_2-independent rundown could be due to dilution of CaM upon excision. Such a dilution of calmodulin has been shown to cause loss of channel inhibition by Ca^{2+} in HERG channels (Schonherr *et al*., 2000). We observed that application of CaM 500 nM did not reverse PIP_2-independent rundown (Figure 3B and C).

Cytosolic application of Mg-ATP prevents PIP_2-independent rundown

MgATP is implicated in the regulation of many ion channels and transporters through a variety of mechanisms (Hilgemann, 1997). We tested the effects of a physiological MgATP concentration on PIP_2-independent rundown. In COS-1 cells, intracellular MgATP concentration has been estimated close to 1 mM (Sippel *et al*., 1997). Co-application of MgATP (1.4 mM) together with PIP_2 entirely abolished the rundown of KCNQ1/KCNE1 channels (Figure 4A). Application of MgATP alone only slowed the rundown process similar to PIP_2, suggesting that the channels require both PIP_2 and MgATP to remain functional. These regulations involve different mechanisms, since only PIP_2-dependent rundown is associated with an accelerated deactivation.

PIP_2 shifts the activation curve of the channel

Prevention by MgATP of PIP_2-independent rundown allowed us to explore the effects of PIP_2 over a longer time of application (tens of minutes are required to study PIP_2 effect on Kir6.2/SUR1 channels; see Figure 4B). In particular, we were able to perform step protocols at different times after patch excision. In COSm6 cells expressing Kir6.2/SUR1 channels, application of 5 μg/ml PIP_2 induced a run-up of the current and a decrease in its ATP sensitivity (Baukrowitz *et al*., 1998; Shyng and Nichols, 1998), consistent with an increase in membrane PIP_2 above the physiological levels. As a control, we successfully reproduced these experiments (Figure 4B) in which the preparation of PIP_2 has been considered as critical (Larsson *et al*., 2000). Then, we performed step protocols in the cell-attached configuration (Figure 4C) and at different time after patch excision in a solution containing PIP_2 in excess (5 μg/ml) and MgATP (1.4 mM; Figure 4D). Examination of the tail current demonstrated a progressive shift in the activation curve towards negative potentials (Figure 4E and F) and a concomitant increase in τ_{deact} (408 ± 55 ms in control versus 552 ± 29 ms with PIP_2; $P < 0.05$; n = 8 and 5). We thus concluded that prolonged application of PIP_2 above physiological concentration altered the KCNQ1/KCNE1 voltage dependency and slowed deactivation.

A model of PIP_2 regulation of Kir6.2/SUR1 channels applies for KCNQ1/KCNE1

Nichols and colleagues have previously proposed a kinetic model that accounts for many observations made on Kir6.2/SUR1 K_{ATP} channels. This model was established on the following observations: (i) the ATP dose–response curve of channel inhibition suggested an ATP binding site for each channel Kir6.2 α-subunit; (ii) the mean open time measured on a single channel did not depend on [ATP]; and (iii) some Kir6.2 pore mutants and PIP_2 application decreased the channel ATP sensitivity (Enkvetchakul *et al*., 2000). We established a similar kinetic model by replacing the regulation of Kir6.2/SUR1 channels by ATP with the regulation of KCNQ1/KCNE1 channels by membrane potential (Figure 5A). The KCNQ1/KCNE1 channel model nicely accounted for our experimental observations, including the effects of PIP_2 on the current amplitude and on the deactivation kinetics with no associated change in the activation kinetics. Like the

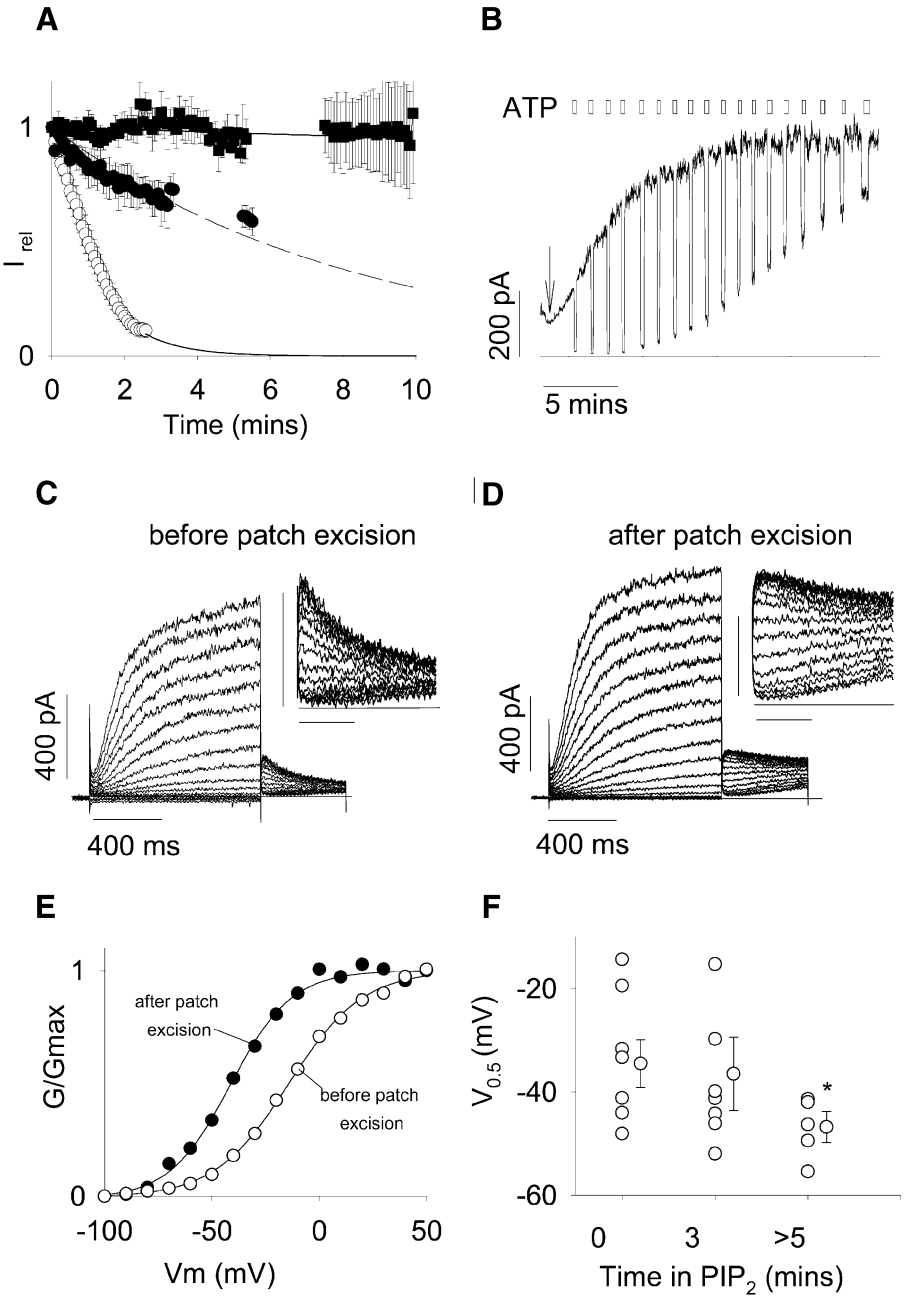

Fig. 4. The effects of PIP_2 on the voltage-dependency of KCNQ1/KCNE1 currents. (**A**) Average time-dependent currents measured at the end of the depolarizing step relative to their maximum value measured after patch excision. Patches were excised in control solution (open circles, $n = 9$), control solution plus 1.4 mM MgATP (0.6 mM free Mg^{2+}; filled circles, $n = 3$), control solution plus 1.4 mM MgATP plus 5 μg/ml PIP_2 (filled squares, $n = 9$) and control solution plus 5 μg/ml PIP_2 (dashed line, $n = 5$). Gaps correspond to acquisition interruptions for other protocols recordings. (**B**) Representative effects of PIP_2 on Kir6.2/SUR1 channels expressed in a COS-7 cell excised patch. PIP_2 was applied as indicated by the arrow. The solid line indicates zero current level. Two hundred micromolar cytosolic ATP repetitive applications are indicated by open boxes. (**C** and **D**) Superimposed KCNQ1/KCNE1 currents recorded when membrane potential was stepped, in 10-mV increments, from a holding potential of –80 mV to various potentials between –100 and +60 mV, and then stepped back to –40 mV. Voltage protocols were performed (C) before and (D) 10 min after patch excision in a MgATP + PIP_2-containing solution. Insets, detail of the tail current at –40 mV. Horizontal bar 200 ms, vertical bar 100 pA. (**E**) Activation curves calculated from the tail current amplitude presented in (C) and (D) before (open circles) and after (filled circles) patch excision in a MgATP + PIP_2-containing solution. (**F**) Potential for half-maximal activation ($V_{0.5}$) calculated from activation curves such as presented in (E) before and at 3 and >5 min after patch excision. $^*P < 0.05$ compared with value at t = 0.

Kir6.2/SUR1 model, the KCNQ1/KCNE1 model is based on the assumption that PIP_2 acts only by stabilizing the open state of the channels (Enkvetchakul *et al*., 2000). We adjusted k_{PIP2} (corresponding to a decrease in PIP_2 levels; Figure 5B) in order to fit the current amplitude at +40 mV at 1, 2 and 3 min after excision. Adjustment of k_{PIP2} constant to rundown data changed the deactivation rate in a way that suitably fitted the experimental deactivation curves (Figure 5C). The KCNQ1/KCNE1 model also showed no change in the activation rate as a function of PIP_2 level, which again was consistent with experimental data. These findings suggest that PIP_2 stabilizes the open

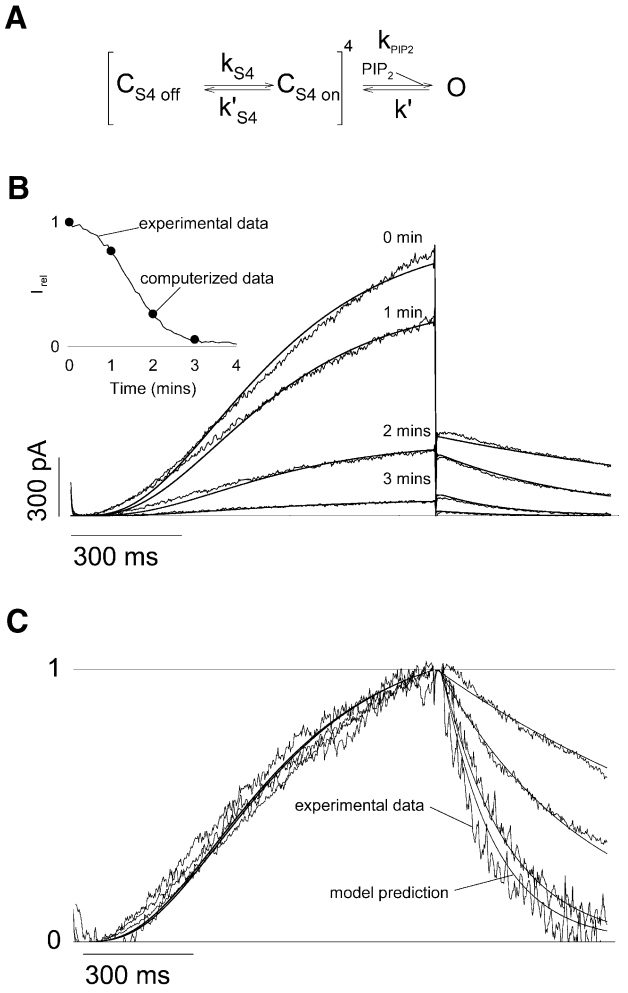

Fig. 5. A model based on the stabilization of the open state by PIP_2 recapitulates the characteristics of the KCNQ1/KCNE1 currents. (**A**) The kinetic scheme presented here is based on previous models of Kir6.2/SUR1 channel regulation by PIP_2. This simple model is based on the assumption that PIP_2 does not affect the voltage sensor (k_{S4}, k'_{S4}), but only a closed state to an open state transition when the four voltage sensors are in the permissive state. Hence k_{S4}, k'_{S4} and k' are PIP_2-independent and only k_{PIP2} varies during the simulated rundown. k_{S4}= 3.56/s during activation and is negligible during deactivation; k'_{S4} = 7.47/s during deactivation and is negligible during activation; and k' = 87.3/s. (**B**) Current traces from Figure 1A, to which the leak current was subtracted, were superimposed with the simulated current (solid lines). k_{PIP2} was fixed to 592.74, 176.43, 25.84 and 4.53/s to best fit the decrease in current amplitude during rundown, as shown in the inset. Inset: simulated (circles) and observed current (solid line) amplitudes as a function of time after patch excision. (**C**) Traces in (B) were normalized to compare the observed and simulated kinetics of activation and deactivation.

state of both a two transmembrane-domain Kir6.2 ATP-gated K^+ channel and a six transmembrane-domain KCNQ1 voltage-gated channel, further strengthening the idea of similar gating processes among potassium channels (Loussouarn *et al*., 2002).

Decreased I_{Ks} current during metabolic poisoning is related to MgATP regulation

In guinea pig cardiomyocytes recorded in the whole-cell configuration, uncoupling of oxidative phosphorylation with dinitrophenol leads not only to activation of the K_{ATP} channel, but also to a decreased activity of a delayed rectifier potassium current (Escande, 1989). I_{Ks} is a major component of the delayed rectifier in guinea pig myocytes (Zicha *et al*., 2003) and may correspond to the component sensitive to metabolic inhibition. We recorded I_{Ks} current in guinea pig cardiac myocytes submitted to dinitrophenol challenge. We initially checked that under our experimental conditions, brief applications of 10 μM dinitrophenol (~30 s) reversibly activated ATP-sensitive K^+ current (not illustrated). Further experiments were then performed in the presence of glibenclamide to prevent K_{ATP} channel activation and also in the presence of E4031 to block the fast component of the delayed rectifier I_{Kr}. Within the same time-frame as required for K_{ATP} channel activation, dinitrophenol led to a reversible inhibition of I_{Ks} by 40.2 ± 9.5% (n = 6). As illustrated in Figure 6, tail current deactivation kinetics were not modified by metabolic poisoning (τ_{deact} = 179.4 ± 24.9 ms in dinitrophenol versus 202 ± 24.9 ms in control; n = 6 and 5, respectively). During metabolic inhibition, MgATP but also PIP_2 decreases (Loussouarn *et al*., 2001). The absence of change in deactivation kinetics in cardiac myocytes suggests that metabolic poisoning affects I_{Ks} through decreased MgATP concentration independently of PIP_2 levels.

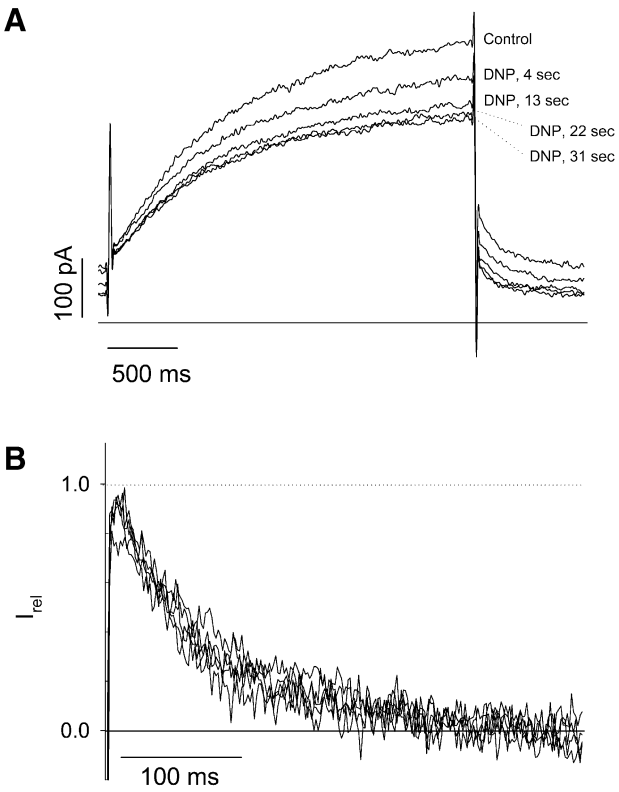

Fig. 6. Metabolic poisoning of cardiomyocytes leads to rundown of I_{Ks}. (**A**) The membrane potential was stepped from a holding potential of –40 to +40 mV (3 s) and then back to –40 mV (1 s), every 4.5 s. Zero current is indicated by a solid line. Cells were perfused permanently with glibenclamide (3 μM), E4031 (0.3 μM) and $CoCl_2$ (1.8 mM) to inhibit I_{KATP}, I_{Kr} and $I_{ca,L}$, respectively. Addition of dinitrophenol (DNP; 10 μM) is followed by a decrease in I_{Ks}. Note the variation of the steady state current at –40 mV, suggesting that another channel may be affected by DNP as well, such as the inward rectifier I_{K1}. (**B**) Normalization of the tail current of I_{Ks} shows no changes in deactivation kinetics.

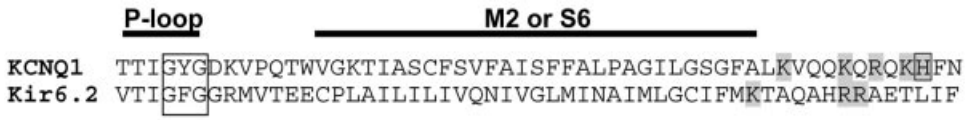

Fig. 7. Alignment of the pore and M2/S6 domains of KCNQ1 with Kir6.2 showing the similar clustering of positive charges at the bottom of the putative pore-lining domains S6 (for KCNQ1) and M2 (for Kir6.2). The boxed histidine is aligned with the KCNQ2 histidine that decreases PIP_2 affinity when neutralized (see text).

Discussion

Dual rundown suggests that two factors are required for functional KCNQ1/KCNE1 channels

The investigation of the rundown process upon patch excision has previously contributed to the identification of many physiological mechanisms involved in ion channels and transporters regulation, including regulation of ion channels by phosphorylation (Becq, 1996). In the present work, we show that KCNQ1/KCNE1 channel activity depends on two distinct intracellular factors. We first unveiled the requirement of PIP_2 to maintain channel activity. In addition, intracellular PIP_2 application uncovered a slower rundown. PIP_2-sensitive rundown and PIP_2-insensitive (but MgATP-sensitive) rundown can easily be distinguished, since only PIP_2-dependent rundown is associated with changes in the channel deactivation kinetics. PIP_2-independent channel rundown could reflect many processes, including the dilution of a cytosolic activator of the channel such as CaM (Schonherr *et al*., 2000), the dephosphorylation of the channel (Sansom *et al*., 1997) or an alteration of the cytoskeleton (Furukawa *et al*., 1996). Intracellular MgATP abolishes PIP_2-independent rundown, which was not affected either by inhibition of the phosphatases usually implicated in channel rundown or by calmodulin application. Although these observations narrow the array of potential mechanisms implicated in KCNQ1/KCNE1 activity, it remains possible that cytoplasmic MgATP participates in many processes, as reviewed by Hilgemann (1997). Additional experiments are required to identify the role of MgATP in maintaining the channel activity.

The bell-shaped effect of intracellular Mg^{2+} on cardiac I_{Ks} current

In guinea pig cardiac cells, whole-cell patch–clamp recordings of the I_{Ks} current carried by KCNQ1/KCNE1 showed a bell-shaped dependence on intracellular Mg^{2+} concentration (Hirahara *et al*., 1998). With 0.03–1 mM $[Mg^{2+}]_i$, I_{Ks} is relatively stable upon patch excision, but decreased rapidly when $[Mg^{2+}]_i$ is below or above this range. These observations can be re-interpreted in the light of the dual regulation of the channel by MgATP and PIP_2. In our experiments, KCNQ1/KCNE1 currents were stable when the intracellular solution contained 5 μg/ml PIP_2 and 1.4 mM MgATP (~0.6 mM free Mg^{2+}, which is in the 0.03–1 mM range). Removing MgATP (Figure 1B, filled squares) or PIP_2 (Figure 4A, filled circles), but also screening PIP_2 by divalent ion application, decreased the KCNQ1/KCNE1 current. Mg^{2+} ion depletion may depress the cardiac I_{Ks} current through a depletion in MgATP. Conversely, high intracellular Mg^{2+} may depress the cardiac I_{Ks} current through the screening of PIP_2 negative charges by divalent cations.

Potential physiological significance of KCNQ1/KCNE1 channel regulation by PIP_2

Recent studies have revealed the implication of PIP_2 in the physiological regulation of ion channels and transporters activity. For example, inhibition of K_{ATP} channels by α1-adrenoceptor stimulation in rat myocytes (Haruna *et al*., 2002) and inhibition of voltage-gated calcium channel by LHRH in bullfrog neurons (Wu *et al*., 2002) are mediated by PIP_2. The requirement of PIP_2 for KCNQ/KCNE1 activity raises the possibility of physiological regulation of the channel complex by receptor-coupled phospholipase C (PLC). In neurons, inhibition of the KCNQ2/KCNQ3 complex by a muscarinic receptor implies PLC and is reversed by PIP_2 (Suh and Hille, 2002; Zhang *et al*., 2003). PLC-coupled receptors are diverse including α1-adrenergic, endothelin or angiotensin II receptors. An orphan receptor APJ is also likely coupled to a PLC (Szokodi *et al*., 2002). Further studies are required to establish a correlation between PLC and KCNQ1/KCNE1 activity. In vestibular dark cells for example, evidence was provided that was consistent with a direct effect of the PKC branch of the PLC pathway on the I_{Ks} current in response to activation of the apical P2U receptor (Marcus *et al*., 1997).

Homologous effect of PIP_2 on a two and a six transmembrane-domain potassium channel

All the data gathered on the effects of PIP_2 on Kir6.2/SUR1 channels can be interpreted by a stabilization of the channel in the open conformation (Enkvetchakul *et al*., 2000). Similarly, our data can also be interpreted by a model based on the stabilization by PIP_2 of the open conformation of KCNQ1/KCNE1 channels. This model is also comparable to Shaker channels kinetic models, i.e. one or more transitions of the four subunits followed by one or more additional concerted transitions (Schoppa and Sigworth, 1998). In the model that we used, one transition of the four subunits and one concerted transition were sufficient to convincingly fit the data. The model illustrates how variations in PIP_2 levels are accompanied by changes in deactivation with no changes in activation kinetics. The requirement of the four domains to be in the 'on' state to allow the channel to finally open makes this transition slow and rate limiting. Since this step is PIP_2-independent (k_{S4} is constant and k'_{S4} negligible), there are no effects of PIP_2 on activation kinetics. On the contrary, deactivation strongly depends on the value of k_{PIP2}: when PIP_2 levels are elevated, k_{PIP2} is much higher than k'_{S4} (592.74 and 7.47/s, respectively), the frequent backwards transitions to the open state slow down deactivation; when PIP_2 levels

are low, k_{PIP2} is much lower, and the channels directly close without backwards transition to the open state.

Similarities between the Kir6.2/SUR1 and KCNQ1/KCNE1 channel models suggest homologous effects of PIP_2 on a six transmembrane-domain, voltage-dependent potassium channel and a two transmembrane-domain, ATP-dependent channel. This homology strengthens the idea that, despite their rather different molecular structure, potassium (and more generally cation) channels share a common fundamental pore architecture (Lu *et al*., 2001; Loussouarn *et al*., 2002). This functional homology may give some insight on the nature of PIP_2 regulation of KCNQ1/KCNE1 channels. Direct interaction of PIP_2 with the C-terminus of several inwardly rectifying K (ROMK, GIRK and IRK) channels has already been shown (Huang *et al*., 1998). An alanine scan (Shyng *et al*., 2000; Cukras *et al*., 2002) of both the C- and N-terminus of Kir6.2 revealed that neutralization of 16 positively charged amino acids (of a total of 38) generally in the near C- and N-termini of Kir6.2 changes the PIP_2 sensitivity of the channel, suggesting that they belong to a potential PIP_2-binding domain and may stabilize the channel open state through electrostatic interaction with membrane PIP_2 (Enkvetchakul *et al*., 2000). This potential PIP_2-binding domain may share the structure of the recently crystallized cytoplasmic pore of GIRK1 (Nishida and MacKinnon, 2002). KCNQ1 presents 17 positively charged amino acids in the N-terminus and 49 in the C-terminus. Identification of the residues implicated in PIP_2 interaction would require a large alanine scan of the channel protein. In favor of the existence of a PIP_2 binding domain in KCNQ1 is the clustering of positive charges at the bottom of M2 and S6 domains of Kir6.2 and KCNQ1, respectively (Figure 7). In Kir6.2, neutralization of these positively charged residues alters the channel PIP_2 sensitivity (Shyng *et al*., 2000), suggesting that they interact electrostatically with PIP_2. The alignment presented in Figure 7 strongly suggests a similar role for the positive amino acids located at the bottom of the S6 domain of KCNQ1, which resembles the M2 domain in Kir6.2 (Lu *et al*., 2001; Loussouarn *et al*., 2002). Interestingly, in KCNQ2/3, neutralization of one histidine in the same region (aligned with the KCNQ1 histidine boxed in Figure 7) leads also to decreased PIP_2 sensitivity (Zhang *et al*., 2003), suggesting that the cluster of positive charges in KCNQ1 may also interact with PIP_2 to stabilize the open state. Much more experiments, including an alanine scan of the 66 positive residues in the C- and N-terminus, are required to clarify the structural homology behind the functional homology.

Materials and methods

Cell isolation, cell culture and cell transfection with KCNQ1/KCNE1 and Kir6.2/SUR1

Single cells were obtained from the heart of guinea pigs by the use of an enzymatic dissociation method as described previously (Baró and Escande, 1989). The concentration of the enzyme used was adjusted to give an activity of 350 U/ml for collagenase (Type I; Sigma) and 0.61 U/ml for protease (Type XIV; Sigma).

The African green monkey kidney-derived cell line COS-7 was obtained from the American Type Culture Collection (Rockville, MD) and cultured in Dulbecco's modified Eagle's medium supplemented with 10% fetal calf serum and antibiotics (100 IU/ml penicillin and 100 μg/ml streptomycin; all from Gibco, Paisley, UK) at 37°C in a humidified incubator. They were subcultured regularly by enzymatic treatment. Cells were transfected when the culture reaches 60–80% confluence, with the plasmids (2 μg per ml of culture medium) complexed with JetPEI (Polyplus-transfection, Strasbourg, France), according to the standard protocol recommended by the manufacturer. The human KCNQ1 and KCNE1 cDNAs were subcloned into the mammalian expression vector, pCI and pCR, respectively (Promega, Madison, WI) under the control of a cytomegalovirus enhancer/promoter. The mouse pCMV-Kir6.2 (Inagaki *et al*., 1995) and the hamster pECE-SUR1 clones were kindly provided by S.Seino and C.G.Nichols, respectively. The plasmid coding for the green fluorescent protein (GFP), used to identify transfected cells was purchased from Clontech. For KCNQ1/KCNE1 current measurement, relative DNA composition was 45% KCNQ1/45% KCNE1/10% GFP. For Kir6.2/SUR1 current measurement, relative DNA composition was 30% Kir6.2/30% SUR1/40% GFP.

Electrophysiology

Twenty-four to 72 h post-transfection, COS-7 cells were mounted on the stage of an inverted microscope and constantly perfused with the Tyrode solution at a rate of 2 ml/min. A microperfusion system allowed local application and rapid change of the different experimental solutions. The bath temperature was maintained at 22.0 ± 1.0°C. Micropipettes (tip resistance 0.8–1.5 MΩ) were pulled from thin-walled glass (Kimble; Vineland, NJ) on a vertical puller (P30; Sutter Instruments, Co., Novato, CA), fire polished, and electrically connected to a patch–clamp amplifier (RK-300; Biologic Science Intruments, Claix, France). Stimulation, data recording and analyses were performed by Acquis1, a software made by Gérard Sadoc (distributed by Biologic Science Intruments) through an analog-to-digital converter (Tecmar TM100 Labmaster; Scientific Solution, Solon, OH, USA). Rundown of KCNQ1/KCNE1 currents as well are activation and deactivation kinetics were studied with a protocol consisting of depolarized voltage steps from a holding potential (–80 mV) to +40 mV (1 s) and then back to –40 mV (500 ms), every 5 s. To better fit the S-shaped activation current, we used the Hodgkin and Huxley model for a voltage-dependent potassium channel activation: $I_k = [1 - \exp(-t/\tau_{act})]^4 \times I_{max}$, with τ_{act} the activation constant, t the time and I_{max} the potassium current amplitude when the channels are fully open (Hille, 2001). KCNQ1/KCNE1 deactivation kinetics were obtained by a monoexponential fit. For the half activation potential ($V_{0.5}$) calculation, the membrane potential was stepped, in 10-mV increments, from a holding potential (–80 mV) to various voltages (pulse potential) between –100 and +60 mV, and then stepped back to –40 mV, where tail currents are visible. The activation curve was obtained from extrapolation of the tail current to the start of the voltage step to avoid contamination with the capacitive current and fitted to a Boltzmann distribution. Kir6.2/SUR1 currents were measured at a membrane potential of –50 mV (pipette voltage = +50 mV). Inward currents at this voltage are shown as positive-going signals.

Whole-cell patch–clamping of cardiomyocytes was described previously (Baró and Escande, 1989). Isolated myocytes were constantly perfused with Tyrode solution maintained at 35 ± 1.0°C. Micropipettes were pulled narrower than in inside-out experiments to reduce intracellular MgATP dilution in the pipette. They had a higher tip resistance (1.5–4 MΩ) when filled with the intracellular solution. Patch–clamp experiments are presented as the mean ± SEM. Statistical significance of the observed effects was assessed by the Student's *t*-test. Off-line analysis was performed using Acquis1 and Microsoft Excel programs. Microsoft Solver was used to fit data by a least-squares algorithm.

Kinetic model of PIP_2 regulation of KCNE1/KCNQ1

Simulations of KCNQ1/KCNE1 currents during rundown were generated from the model presented in Figure 5A. KCNQ1/KCNE1 currents during a depolarizing step are based on the assumption that all the S4 domains are in the 'off' conformation ($C_{s4\ off} = 1$, $C_{s4\ on} = 0$ and $O = 0$) at the beginning of the depolarizing step. KCNQ1/KCNE1 tail currents during repolarization are calculated from the Po value obtained at the end of the depolarizing step. Only k_{PIP2} is PIP_2 dependent and its values during the simulated rundown were chosen to best fit the decrease in the maximal current amplitude at 40 mV during rundown (cf. legend of Figure 5). Microsoft Excel was used to perform the currents simulation.

Solutions and drugs

The pipette (extracellular) solution used in experiments on transfected COS-7 cells had the following composition: 145 mM Na-gluconate, 4 mM K-gluconate, 4 mM $Mg_{1/2}$-gluconate (1 mM free Mg^{2+}), 7 mM $Ca_{1/2}$-gluconate (1 mM free Ca^{2+}), 5 mM K-HEPES, 1 mM K-EGTA, pH 7.4 with NaOH. The standard microperfusion (intracellular) solution

contained 145 mM K-gluconate, 10 mM K-HEPES, 1 mM K-EGTA, pH 7.2 with NaOH, with additions as described. The pipette (intracellular) solution used in experiments on cardiomyocytes cells had the following composition (in mM): K-gluconate 120, KCl 15, HEPES 5, EGTA 5. The local perfusion contained (in mM): NaCl 132, KCl 4, HEPES 10, mannitol 20 and glucose 5, $MgCl_2$ 1.2, $CoCl_2$ 1.8 and E4031 0.3 μM, glibenclamide 3 μM. Metabolic inhibition was performed by replacing glucose by 10 μM dinitrophenol. Free activities were calculated using a software designed by G.L.Smith (University of Glasgow, Glasgow, UK). PIP_2 (Roche Molecular Biochemical) was sonicated in ice for 30 min before application to inside-out patches. Okadaic acid and CaM (Calbiochem) containing solution were prepared from stock solution in water stored at –20°C (300 and 50 μM, respectively). All other products were purchased from Sigma.

Acknowledgements

We thank Aziza El Harchi, Béatrice Leray and Marie-Joseph Louerat for expert technical assistance. This work was supported by grants from the Institut National de la Santé et de la Recherche Médicale (INSERM). G.L. and I.B. are recipients of tenure positions supported by the Centre National de la Recherche Scientifique (CNRS). F.C. is a recipient of a tenure position supported by the Institut National de la Santé et de la Recherché Médicale (INSERM).

References

Barhanin,J., Lesage,F., Guillemare,E., Fink,M., Lazdunski,M. and Romey,G. (1996) K(V)LQT1 and lsK (minK) proteins associate to form the I(Ks) cardiac potassium current. *Nature*, **384**, 78–80.

Baró,I. and Escande,D. (1989) A long lasting Ca^{2+}-activated outward current in guinea-pig atrial myocytes. *Pflugers Arch.*, **415**, 63–71.

Baukrowitz,T and Fakler,B. (2000) K(ATP) channels: linker between phospholipid metabolism and excitability. *Biochem. Pharmacol.*, **60**, 735–740.

Baukrowitz,T., Schulte,U., Oliver,D., Herlitze,S., Krauter,T., Tucker,S.J. Ruppersberg,J.P. and Fakler,B. (1998) PIP_2 and PIP as determinants for ATP inhibition of K_{ATP} channels. *Science*, **282**, 1141–1144.

Becq,F. (1996) Ionic channel rundown in excised membrane patches. *Biochim. Biophys Acta*, **1286**, 53–63.

Bian,J., Cui,J. and McDonald,T.V. (2001) HERG K^+ channel activity is regulated by changes in phosphatidyl inositol 4,5-bisphosphate. *Circ. Res.*, **89**, 1168–1176.

Cukras,C.A., Jeliaskova,I. and Nichols,C.G. (2002) Structural and functional determinants of conserved lipid interaction domains of inward rectifying Kir6.2 channels. *J. Gen. Physiol.*, **119**, 581–591.

Enkvetchakul,D., Loussouarn,G., Makhina,E., Shyng,S.L. and Nichols,C.G. (2000) The kinetic and physical basis of K(ATP) channel gating: toward a unified molecular understanding. *Biophys. J.*, **78**, 2334–2348.

Escande,D. (1989) The pharmacology of ATP-sensitive K^+ channels in the heart. *Pflugers Arch.*, **414**, S93–S98.

Furukawa,T., Yamane,T., Terai,T, Katayama,Y. and Hiraoka M. (1996) Functional linkage of the cardiac ATP-sensitive K^+ channel to the actin cytoskeleton. *Pflugers Arch.*, **431**, 504–512.

Grunnet,M., Jespersen,T., MacAulay,N., Jorgensen,N.K., Schmitt,N., Pongs,O., Olesen,S.P. and Klaerke,D.A. (2003) KCNQ1 channels sense small changes in cell volume. *J. Physiol.*, **549**, 419–427.

Haruna,T., Yoshida,H., Nakamura,T.Y., Xie,L.H., Otani,H., Ninomiya,T., Takano,M., Coetzee,W.A. and Horie,M. (2002) Alpha1-adrenoceptor-mediated breakdown of phosphatidylinositol 4,5-bisphosphate inhibits pinacidil-activated ATP-sensitive K+ currents in rat ventricular myocytes. *Circ. Res.*, **91**, 232–239.

Hilgemann,D.W. (1997) Cytoplasmic ATP-dependent regulation of ion transporters and channels: mechanisms and messengers. *Annu. Rev. Physiol.*, **59**, 193–220.

Hilgemann,D.W., Feng,S. and Nasuhoglu,C. (2001) The complex and intriguing lives of PIP2 with ion channels and transporters. *Sci. STKE*, **111**, RE19.

Hille,B. (2001) *Ion Channels of Excitable Membranes*. Sinauer, Sunderland, MA.

Hirahara,K., Matsubayashi,T., Matsuura,H. and Ehara,T. (1998) Intracellular Mg^{2+} depletion depresses the delayed rectifier K^+ current in guinea pig ventricular myocytes. *Jpn. J. Physiol.*, **48**, 81–89.

Huang,C.L., Feng,S. and Hilgemann,D.W. (1998) Direct activation of inward rectifier potassium channels by PIP2 and its stabilization by Gβγ. *Nature*, **391**, 803–806.

Inagaki,N., Gonoi,T., Clement,J.P., Namba,N., Inazawa,J., Gonzalez,G., Aguilar-Bryan,L., Seino,S. and Bryan,J. (1995) Reconstitution of IKATP: an inward rectifier subunit plus the sulfonylurea receptor. *Science*, **270**, 1166–1170.

Larsson,O., Barker,C.J. and Berggren,P.O. (2000) Phosphatidylinositol 4,5-bisphosphate and ATP-sensitive potassium channel regulation: a word of caution. *Diabetes*, **49**, 1409–1412.

Loussouarn,G., Pike,L.J., Ashcroft,F.M., Makhina,E.N. and Nichols,C.G. (2001) Dynamic sensitivity of ATP-sensitive K^+ channels to ATP. *J. Biol. Chem.*, **276**, 29098–29103.

Loussouarn,G., Rose,T. and Nichols,C.G. (2002) Structural basis of inward rectifying potassium channel gating. *Trends Cardiovasc. Med.*, **12**, 253–258.

Lu,Z., Klem,A.M. and Ramu,Y. (2001) Ion conduction pore is conserved among potassium channels. *Nature*, **413**, 809–813.

Marcus,D.C., Sunose,H, Liu,J., Shen,Z. and Scofield,M.A. (1997) P2U purinergic receptor inhibits apical IsK/KvLQT1 channel via protein kinase C in vestibular dark cells. *Am. J. Physiol.*, **273**, C2022–C2029.

Marx,S.O., Kurokawa,J., Reiken,S., Motoike,H., D'Armiento,J., Marks,A.R. and Kass,R.S. (2002) Requirement of a macromolecular signaling complex for beta adrenergic receptor modulation of the KCNQ1–KCNE1 potassium channel. *Science*, **295**, 496–499.

Nishida,M. and MacKinnon,R. (2002) Structural basis of inward rectification. Cytoplasmic pore of the G protein-gated inward rectifier GIRK1 at 1.8 Å resolution. *Cell*, **111**, 957–965.

Potet,F., Scott,J.D., Mohammad-Panah,R., Escande,D. and Baro,I. (2001) AKAP proteins anchor cAMP-dependent protein kinase to KvLQT1/IsK channel complex. *Am. J. Physiol.*, **280**, H2038–H2045.

Sanguinetti,M.C., Curran,M.E., Zou,A., Shen,J., Spector,P.S., Atkinson,D.L. and Keating,M.T. (1996) Coassembly of K(V)LQT1 and minK (IsK) proteins to form cardiac I(Ks) potassium channel. *Nature*, **384**, 80–83.

Sansom,S.C., Stockand,J.D., Hall,D. and Williams,B. (1997) Regulation of large calcium-activated potassium channels by protein phosphatase 2A. *J. Biol. Chem.*, **272**, 9902–9906.

Schonherr,R., Lober,K. and Heinemann,S.H. (2000) Inhibition of human ether a go-go potassium channels by Ca^{2+}/calmodulin. *EMBO J.*, **19**, 3263–3271.

Schoppa,N.E. and Sigworth,F.J. (1998) Activation of Shaker potassium channels. III. An activation gating model for wild-type and V2 mutant channels. *J. Gen. Physiol.*, **111**, 313–342.

Shen,Z. and Marcus,D.C. (1998) Divalent cations inhibit IsK/KvLQT1 channels in excised membrane patches of strial marginal cells. *Hear. Res.*, **123**, 157–167.

Shyng,S.L. and Nichols,C.G. (1998) Membrane phospholipid control of nucleotide sensitivity of KATP channels. *Science*, **282**, 1138–1141.

Shyng,S.L., Cukras,C.A., Harwood,J. and Nichols,C.G. (2000) Structural determinants of PIP2 regulation of inward rectifier KATP channels. *J. Gen. Physiol.*, **116**, 599–607.

Sippel,C.J., Dawson P.A., Shen T. and Perlmutter D.H. (1997) Reconstitution of bile acid transport in a heterologous cell by cotransfection of transporters for bile acid uptake and efflux. *J. Biol. Chem.*, **272**, 18290–18297.

Suh,B.C. and Hille,B. (2002) Recovery from muscarinic modulation of M current channels requires phosphatidylinositol 4,5-bisphosphate synthesis. *Neuron*, **35**, 507–520.

Szokodi,I. *et al*. (2002) Apelin, the novel endogenous ligand of the orphan receptor APJ, regulates cardiac contractility. *Circ. Res.*, **91**, 434–440.

Towbin,J.A. and Vatta,M. (2001) Molecular biology and the prolonged QT syndromes. *Am. J. Med.*, **110**, 385–398.

Tristani-Firouzi,M. and Sanguinetti,M.C. (1998) Voltage-dependent inactivation of the human K^+ channel KvLQT1 is eliminated by association with minimal K^+ channel (minK) subunits. *J. Physiol.*, **510**, 37–45.

Vetter,D.E. *et al*. (1996) Inner ear defects induced by null mutation of the isk gene. *Neuron*, **17**, 1251–1264.

Wen,H. and Levitan,I.B. (2002) Calmodulin is an auxiliary subunit of KCNQ2/3 potassium channels. *J. Neurosci.*, **22**, 7991–8001.

Wu,L., Bauer,C.S., Zhen,X.G., Xie,C. and Yang,J. (2002) Dual regulation of voltage-gated calcium channels by PtdIns(4,5)P2. *Nature*, **419**, 947–952.

Yang,Y. and Sigworth,F.J. (1998) Single-channel properties of IKs potassium channels. *J. Gen. Physiol.*, **112**, 665–678.

Yin,H.L. and Janmey,P.A. (2003) Phosphoinositide regulation of the actin cytoskeleton. *Annu. Rev. Physiol.*, **65**, 761–789.

Yus-Najera,E., Santana-Castro,I. and Villarroel,A. (2002). The identification and characterization of a noncontinuous calmodulin-binding site in noninactivating voltage-dependent KCNQ potassium channels. *J. Biol. Chem.*, **277**, 28545–28553.

Zhang,H., Craciun,L.C., Mirshahi,T., Rohacs,T., Lopes,C.M., Jin,T. and Logothetis,D.E. (2003) PIP_2 activates KCNQ channels and its hydrolysis underlies receptor-mediated inhibition of M currents. *Neuron*, **37**, 963–975.

Zicha,S., Moss,I., Allen,B., Varro,A., Papp,J., Dumaine,R., Antzelevitch,C. and Nattel,S. (2003) Molecular basis of species-specific expression of repolarizing potassium currents in the heart. *Am. J. Physiol.*, **285**, H1641–H1649.

Received January 13, 2003; revised July 21, 2003; accepted August 21, 2003